Jacques Bélair · Ian A. Frigaard
Herb Kunze · Roman Makarov
Roderick Melnik · Raymond J. Spiteri *Editors*

Mathematical and Computational Approaches in Advancing Modern Science and Engineering

Springer

Mathematical and Computational Approaches in Advancing Modern Science and Engineering

Jacques Bélair • Ian A. Frigaard • Herb Kunze
Roman Makarov • Roderick Melnik
Raymond J. Spiteri
Editors

Mathematical and Computational Approaches in Advancing Modern Science and Engineering

Springer

Editors
Jacques Bélair
Department of Mathematics and Statistics
University of Montreal
Montreal, QC
Canada

Ian A. Frigaard
Department of Mathematics
University of British Columbia
Vancouver, BC
Canada

Herb Kunze
Department of Mathematics and Statistics
University of Guelph
Guelph, ON
Canada

Roman Makarov
Department of Mathematics
Wilfrid Laurier University
Waterloo, ON
Canada

Roderick Melnik
MS2Discovery Institute
Wilfrid Laurier University
Waterloo, ON
Canada

Raymond J. Spiteri
Department of Computer Science
University of Saskatchewan
Saskatoon, SK
Canada

ISBN 978-3-319-30377-2 ISBN 978-3-319-30379-6 (eBook)
DOI 10.1007/978-3-319-30379-6

Library of Congress Control Number: 2016943639

Mathematics Subject Classification (2010): 00A69, 00A71, 00A79, 92-XX, 35Qxx, 81T80, 97M10, 47N60, 49-xx, 91Axx, 62Pxx, 97Pxx, 70-xx

Printed on acid-free paper

This Springer imprint is published by Springer Nature
The registered company is Springer International Publishing AG Switzerland

Preface

This book consists of five parts covering a wide range of topics in applied mathematics, modeling, and computational science (AMMCS). It resulted from two highly successful meetings held jointly in Waterloo (Canada) on the main campus of Wilfrid Laurier University. It is the oldest university in the Cambridge-Kitchener-Waterloo-Guelph area, a beautiful part of Canada, just west of the city of Toronto. The main campus of the university is located in a comfortable driving distance from some of North America's most spectacular tourist destinations, including the Niagara Escarpment, a UNESCO World Biosphere Reserve. Over the years, this university has become a traditional venue for the International Conference on Applied Mathematics, Modeling and Computational Science, and in 2015 it was held jointly with the annual meeting of the Canadian Applied and Industrial Mathematics (CAIMS) from June 7–12, 2015. The AMMCS interdisciplinary conference series runs biannually. Focusing on recent advances in applied mathematics, modeling, and computational science, the 2015 AMMCS-CAIMS Congress drew some of the top scientists, mathematicians, engineers, and industrialists from all over the world and was a true celebration of interdisciplinary research and collaboration involving mathematical, statistical, and computational sciences within a larger international community.

The book clearly demonstrates the importance of interdisciplinary interactions between mathematicians, scientists, engineers, and representatives from other disciplines. It is a valuable source of the methods, ideas, and tools of mathematical modeling, computational science, and applied mathematics developed for a variety of disciplines, including natural and social sciences, medicine, engineering, and technology. Original results are presented here on both fundamental and applied levels, with an ample number of examples emphasizing the interdisciplinary nature and universality of mathematical modeling.

The book contains 70 articles, arranged according to the following topics represented by five parts:

- Theory and Applications of Mathematical Models in Physical and Chemical Sciences

Fig. 1 Participants of the 2015 International AMMCS-CAIMS Congress, Canada (Photo taken by Tomasz Adamski on the Waterloo Campus at Wilfrid Laurier University)

- Mathematical and Computational Methods in Life Sciences and Medicine
- Computational Engineering and Mathematical Foundation, Numerical Methods, and Algorithms
- Mathematics and Computation in Finance, Economics, and Social Sciences
- New Challenges in Mathematical Modeling for Scientific and Engineering Applications

These chapters are based on selected refereed contributions made by the participants of both meetings. The AMMCS-CAIMS Congress featured over 30 special and contributed sessions with mini-symposia ranging from mathematical models in nanoscience and nanotechnology to statistical equilibrium in economics and to mathematical neuroscience, the embedded Conference of the Computational Fluid Dynamics Society of Canada, and the 2nd Canadian Symposium on Scientific Computing and Numerical Analysis, as well as larger sessions around such scientific themes as applied analysis and dynamical systems, industrial mathematics, mathematical biology, financial mathematics, and much more. Over 600 participants from all continents attended the Congress and shared the latest achievements, ideas, insights, and theories about modern problems in science, engineering, and society that can be approached with new advances in mathematical modeling and mathematical, computational, and statistical methods.

This book presents a selected sample of the above topics and can serve as a reference to some of the state-of-the-art original works on a range of such topics. It

Fig. 2 Members of the local organizing committee and student volunteers (Photo taken by Dr. Shyam Badu on the Waterloo Campus at Wilfrid Laurier University)

has a strong multidisciplinary focus, supported by fundamental theories, rigorous procedures, and examples from applications. Furthermore, the book provides a multitude of examples accessible to graduate students and can serve as a source for graduate student projects.

Taking this opportunity, we would like to thank our colleagues on the AMMCS-CAIMS Congress organizing team, as well as our sponsors and partners, in particular the Fields Institute and PIMS, and the Centre de Recherches Mathématiques, as well as Wilfrid Laurier University, NSERC, and the Government of Ontario. Among others, traditional supporters of the AMMCS Interdisciplinary Conference series were Maplesoft and SHARCNET, as well as Springer, De Gruyter, and CRC Press. The Congress was held under the auspices of the MS2Discovery Interdisciplinary Research Institute based at Wilfrid Laurier University and in cooperation with the Society of Industrial and Applied Mathematics and the American Institute of Mathematical Sciences.

The Congress scientific committee included 15 internationally known researchers. We would like to thank them, as well as the Congress referees whose help in the refereeing process was invaluable. Among them we had some of the leading researchers from all parts of the world, and their assistance was decisive in completing this project. Our technical support committee and students' team were exemplary, and we are truly grateful for their efforts. Last but not least, we are also grateful to the editorial team at Springer, in particular Martin Peters and Ruth Allewelt, whose continuous support during the entire process was at the highest professional level.

We believe that the book will be a valuable addition to the libraries, as well as to private collections of university researchers and industrialists, scientists and engineers, graduate students, and all of those who are interested in the recent progress in mathematical modeling and mathematical, computational, and statistical methods applied in interdisciplinary settings.

Montreal, Canada	Jacques Bélair
Vancouver, Canada	Ian Frigaard
Guelph, Canada	Herb Kunze
Waterloo, Canada	Roman Makarov
Waterloo, Canada	Roderick Melnik
Saskatoon, Canada	Raymond Spiteri

Contents

Part III Computational Engineering and Mathematical Foundation, Numerical Methods and Algorithms

Part I
Theory and Applications of Mathematical Models in Physical and Chemical Sciences

Compressibility Coefficients in Nonlinear Transport Models in Unconventional Gas Reservoirs

Iftikhar Ali, Bilal Chanane, and Nadeem A. Malik

Abstract Transport models for gas flow in unconventional hydrocarbon reservoirs possess several model parameters such as the density (ρ), the permeability (K), the Knudsen number (K_n), that are strongly dependent upon the pressure p. Each physical parameter, say γ, in the system has an associated compressibility factor $\zeta_\gamma = \zeta_\gamma(p)$ (which is the relative rate of change of the parameter with respect to changes in the pressure, Ali I et al. (2014, Time-fractional nonlinear gas transport equation in tight porous media: an application in unconventional gas reservoirs. In: 2014 international conference on fractional differentiation and its applications (ICFDA), Catania, pp 1–6, IEEE)). Previous models have often assumed that $\zeta_\gamma = Const$, such as Cui (Geofluids 9(3):208–223, 2009), and Civan (Transp Porous Media 86(3):925–944, 2011). Here, we investigate the effect of selected compressibility factors (real gas deviation factor (ζ_Z), gas density (ζ_ρ), gas viscosity (ζ_μ), permeability (ζ_K), and the porosity (ζ_ϕ) of the source rock) as functions of the pressure upon rock properties such as K and ϕ. We also carry out a sensitivity analysis to estimate the importance of each model parameter. The results are compared to available data.

1 Introduction

Unconventional gas reservoirs include tight gas, coalbed methane, and shale gas. Shale gas is distributed over large areas and is found in discrete largely unconnected gas pockets. Different methods are applied to induce fractures inside the rocks to release the gas, such as hydraulic fracturing, but this is very expensive. Hence, an initial guess is required before drilling. Reservoir simulations can be crucial in

I. Ali (✉) • B. Chanane • N.A. Malik
Department of Mathematics & Statistics, King Fahd University of Petroleum and Minerals, P. O. Box 5046, Dhahran 31261, Saudi Arabia
e-mail: namalik@kfupm.edu.sa; nadeem_malik@cantab.net; chanane@kfupm.edu.sa; iali@kfupm.edu.sa

J. Bélair et al. (eds.), *Mathematical and Computational Approaches in Advancing Modern Science and Engineering*, DOI 10.1007/978-3-319-30379-6_1

assisting this process for economical recovery. This requires accurate determination of fluid and rock properties, and a realistic transport model, [2, 5, 11, 15].

Unconventional gas reservoirs are characterized by extremely low permeability, in the nano- to micro-Darcy range, and low porosity, in the 4 %–15 % range. The gas extraction process is very complex and involves new technologies, and takes a lot of time, money and human resources, [18]. The science and technology of tight gas transport and extraction is still in its infancy, and field data urgently required especially from shale gas reservoirs in order to test the newly emerging theories.

Reservoir simulations typically solve model transport equations in the form of advection-diffusion partial differential equations (PDE). Some of the latest models are highly non-linear, where the apparent diffusivity $D(p)$ and the apparent velocity $U(p, p_x)$ are strongly non-linear functions of the pressure and its derivative, [7]. D and U involve compressibility factors ζ_γ of various physical parameters,

$$\zeta_\gamma = \frac{\partial \ln \gamma}{\partial p} = \frac{1}{\gamma}\frac{\partial \gamma}{\partial p}. \tag{1}$$

and these must be known as functions of p and p_x. However, most applications to date have been simplified by assuming constant compressibility factors. The impact of this important assumption has not been assessed to date.

The aim here is to assess the importance of using fully pressure dependent model parameters. This is done through numerical simulations of the transport equation and matching the results against the data from Pong et al. [17]. A sensitivity analysis is also carried out to assess the importance of each physical parameter in the system.

2 Physical Properties of Shale Gas Reservoirs

Various flow regimes occur in the gas transport process through tight shale rock formations [10]. They are classified by a Knudsen number, see Table 1 and [17, 19], which is the ratio of mean free path of gas molecules (λ) to the radius (R) of the flow channels, $K_n = \lambda/R$. λ is given by [13], $\lambda = \frac{\mu}{\rho}\sqrt{\frac{\pi}{2R_gT}}$, where ρ is gas density, T is temperature, R_g is universal gas constant, and μ is gas viscosity. R is given by, [4, 6], $R = 2\sqrt{2\tau}\sqrt{\frac{K}{\phi}}$, where τ is the tortuosity and ϕ is the porosity of porous media and K is intrinsic permeability. Several recent works have focused transport on the so-called four flow regimes, Table 1.

Table 1 Classification of flow regimes based on Knudsen number, [19]

Knudsen number	Flow regimes
$K_n < 0.01$	Continuous flow
$0.01 < K_n < 0.1$	Surface diffusion or slip flow
$0.1 < K_n < 10$	Transition flow
$K_n > 10$	Knudsen diffusion or free molecular flow

The correlation between porosity and intrinsic permeability is given by the Kozeny-Carman equation [8]

$$\sqrt{\frac{K}{\phi}} = \Gamma_{KC}\left(\frac{\phi}{\alpha_{KC} - \phi}\right)^{\beta_{KC}}, \tag{2}$$

where $\phi < \alpha_{KC} \leq 1$, $0 \leq \beta_{KC} < \infty$ and $\Gamma_{KC} \geq 0$. α_{KC}, β_{KC}, and Γ_{KC} are empirical constants which must be determined, or estimated, before hand.

For the simulation purposes, we use the following porosity-pressure correlation,

$$\phi = a_\phi \exp(-b_\phi p^{c_\phi}), \tag{3}$$

where a_ϕ, b_ϕ and c_ϕ are model constants. Tortuosity is related to porosity by,

$$\tau = 1 + a_\tau(1 - \phi), \tag{4}$$

where a_τ is also a model constant.

There is a difference between the intrinsic permeability, K, and the apparent permeability, K_a. K is the measured permeability from rock samples, but due to various physical effects such as slip flow, the quantity appearing in transport equations is K_a. Beskok [3] has derived an formula that relates the two quantities,

$$K_a = Kf(K_n) \tag{5}$$

where $f(K_n)$ is the flow condition function given by

$$f(K_n) = (1 + \sigma K_n)\,(1 + (4 - b_{SF})K_n)\,(1 - b_{SF}K_n)^{-1}, \tag{6}$$

where σ is called the Rarefaction Coefficient Correlation [6] given by

$$\sigma = \sigma_o\left(1 + A_\sigma K_n^{-B_\sigma}\right)^{-1}, \tag{7}$$

where A_σ and B_σ are empirical constants and b_{SF} in Eq. 6 is the slip factor.

Some of the gas adheres (clings) to pore surfaces due to the diffusion of gas molecules. Cui [9] and Civan [7] developed a formula for estimating the amount of adsorbed gas based on Langmuir isotherms and is given by

$$q = \frac{\rho_s M_g}{V_{std}} q_a = \frac{\rho_s M_g}{V_{std}} \frac{q_L p}{p_L + p}, \tag{8}$$

where ρ_s (kg/m^3) denotes the material density of the porous sample, q (kg/m^3) is the mass of gas adsorbed per solid volume, q_a (std m^3/kg) is the standard volume of gas adsorbed per solid mass, q_L (std m^3/kg) is the Langmuir gas volume, V_{std} (std m^3/kmol) is the molar volume of gas at standard temperature (273.15 K) and pressure (101,325 Pa), p (Pa) is the gas pressure, p_L (Pa) is the Langmuir gas pressure, and M_g (kg/kmol) is the molecular weight of gas.

Gas density ρ (kg/m^3) is given by the real-gas equation of state,

$$\rho = \frac{M_g p}{Z R_g T} \tag{9}$$

where Z (dimensionless) is the real gas deviation factor [12] and it can be found by using the correlation developed by Mahmoud [14] and it is given by

$$Z = a p_r^2 + b p_r + c \tag{10}$$

$$a = 0.702 \exp(-2.5 t_r) \tag{11}$$

$$b = -5.524 \exp(-2.5 t_r) \tag{12}$$

$$c = 0.044 T_r^2 - 0.164 t_r + 1.15 \tag{13}$$

where p_c is the critical pressure and t_c is the critical temperature, and $p_r = p/p_c$ and $t_r = t/t_c$ are the reduced pressure and temperature respectively.

Mahmoud [14] also gave correlations for determining the gas viscosity,

$$\mu = \mu_{S_c} \exp(A \rho^B) \tag{14}$$

$$A = 3.47 + 1588 T^{-1} + 0.0009 M_g$$

$$B = 1.66378 - 0.04679 A$$

$$\mu_{S_c} = \frac{1}{(10.5)^4} \left[\frac{M^3 p_c^4}{T_c} \right]^{1/6} \times \left[0.807 T_r^{0.618} - 0.357 \exp(0.449 T_r) + 0.34 \exp(-4.058 T_r) + 0.018 \right]$$

3 Mathematical Formulation

The ultra low permeability and the occurrence of various flow regimes are key features of unconventional gas reservoirs (UGR). The PDE's that are used to describe transport process in conventional gas reservoirs (CGR) are based on Darcy's law $u = (-K/\mu)dp/dx$ and continuity equation $-(\rho u)_x = 0$, where K, μ, and ρ are constants, but such models do not produce satisfactory results in UGRs. Civan [7] has proposed a transport model for gas flow through tight porous media which incorporates all flow regimes that occur in the reservoirs. Civan's model is a non-linear advection-diffusion PDE for the pressure field $p(x, t)$, which is given by,

$$\frac{\partial p}{\partial t} + U(p, p_x)\frac{\partial p}{\partial x} = D(p)\frac{\partial^2 p}{\partial x^2}. \tag{15}$$

The apparent diffusivity D (m^2/s) is given by,

$$D = \frac{\rho K_a}{\mu}\left\{\rho\phi\zeta_1(p) + (1-\phi)q\zeta_2(p)\right\}^{-1}, \tag{16}$$

and the apparent convective flux (velocity) U (m/s) is given by,

$$U = -\zeta_3(p)D\frac{\partial p}{\partial x}. \tag{17}$$

where the ζ_1, ζ_2 and ζ_3 appearing in D and U are given by

$$\zeta_1(p) = \zeta_\rho(p) + \zeta_\phi(p), \tag{18}$$

$$\zeta_2(p) = \zeta_q(p) - \left(\frac{\phi}{1-\phi}\right)\zeta_\phi(p), \tag{19}$$

$$\zeta_3(p) = [\zeta_\rho(p) + \zeta_{K_a}(p) - \zeta_\mu(p)]. \tag{20}$$

where $\zeta_{K_a} = \zeta_K + \zeta_f$ which is obtained from Eq. (5).

A numerical solver for the system equations (15), (16), (17), (18), (19), and (20) has been developed. We use a finite volume implicit method with constant grid size and constant time step. The system is linearised and iterated to convergence before advancing to the next time step. The implicit nature of the solver gives stability to the solver which is essential for such a highly non-linear system. The solver can also be applied to the steady state system, see below.

4 Model Validation Under Steady State Conditions

The steady state solution for the pressure field is obtained by solving, (see [1, 7]),

$$L_a\left(\frac{\partial p}{\partial x}\right) = \frac{\partial^2 p}{\partial x^2}, \qquad 0 \le x \le L, \tag{21}$$

where

$$L_a = -\left[\zeta_\rho(p) + \zeta_K(p) + \zeta_f(p) - \zeta_\mu(p)\right]\frac{\partial p}{\partial x}, \tag{22}$$

with boundary conditions, $p(0) = p_L$ and $p(L) = p_R$; p_L and p_R assumed known.

Sixteen different models were considered, Table 2. An entry of '0' means that the compressibility factor is zero, $\zeta_\gamma = 0$; an entry of 'p' means that $\zeta_\gamma \neq 0$ and the associated physical parameter is a function of pressure, $\gamma = \gamma(p)$. The final column shows the relative error between the simulated values and the experimental values of Pong et al. [16], given by,

$$\text{Relative Error} = \sum_{i=1}^{N}\left[\frac{p_i^{cal} - p_i^{meas}}{p_i^{cal}}\right]^2. \tag{23}$$

where the summation is over the $N = 30$ data-points in [16]. Case 1 in Table 2 corresponds to the Darcy law where all the physical parameters are constant and

Table 2 List of models considered. In columns 2–5, an entry of 0 means that the compressibility factor is zero; an entry of p means that it is nonzero and the associated physical parameter is function of pressure p. The final column shows the relative error from simulations using Eq. (23)

Cases	ζ_ρ	ζ_K	ζ_f	ζ_μ	Error
1	0	0	0	0	2.69e−02
2	p	0	0	0	2.68e−02
3	0	p	0	0	4.05e−03
4	0	0	p	0	3.16e−01
5	0	0	0	p	2.69e−02
6	p	p	0	0	1.17e−01
7	p	0	p	0	3.19e−02
8	p	0	0	p	2.68e−02
9	0	p	p	0	1.84e+00
10	0	p	0	p	4.05e−03
11	0	0	p	p	3.17e−01
12	p	p	p	0	1.37e−04
13	p	p	0	p	1.17e−01
14	0	p	p	p	3.19e−02
15	p	0	p	p	1.84e+00
16	p	p	p	p	1.36e−04

$\zeta_\gamma = 0$. Case 16 is the fully pressure-dependent case. An additional case, from Civan [8] with constant factors for ζ_K, ζ_ϕ, ζ_μ, and ζ_τ, was also carried out.

Figure 1 shows the comparisons of the simulated results (solid lines) for the pressure against the distance for selected models (see captions) against the data of Pong et al. [16] (symbols). The inlet pressures for the different simulations are, respectively from bottom to top, 135, 170, 205, 240, and 275 kPa. Figure 1a compares with Darcy's Law Case 1, and it shows significant errors. Figure 1b compares with Civan's case, and Fig. 1c compares with Case 16, which is the best fit to the data. Figure 1d shows the relative error on log-scale for the 16 cases in Table 2. We refer to Case 16 as the Base Case henceforth (Table 3).

It is important to note that although the Civan case Fig. 1b and the Base Case Fig. 1c appear to yield similar results, the rock properties obtained in the two cases are quite different. Civan used $\phi = 0.2$ independent of pressure and he predicted

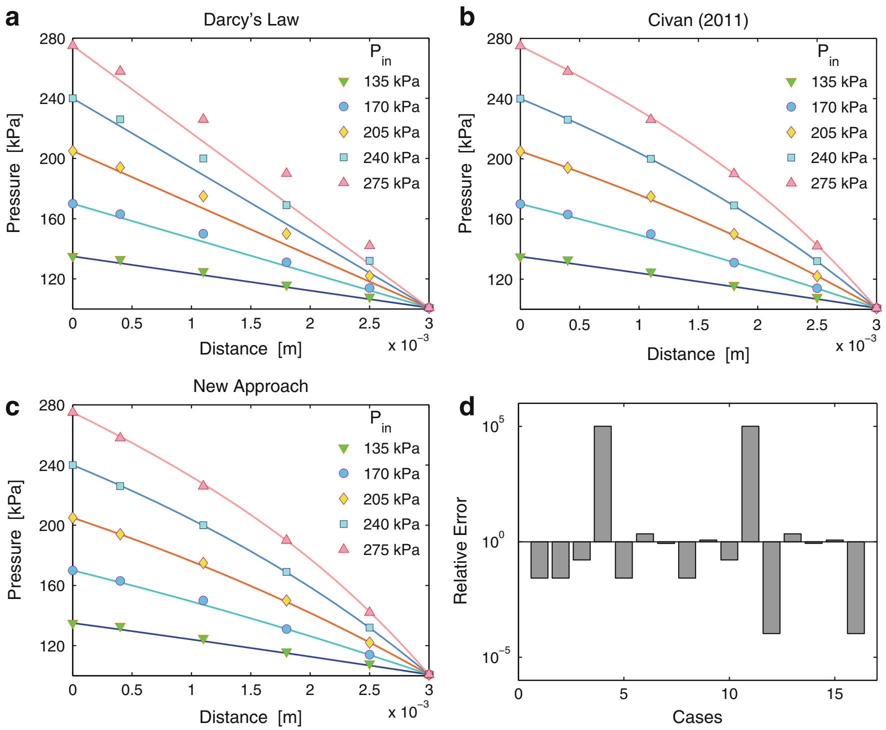

Fig. 1 Pressure, p against the distance along the core sample, x, from numerical solutions of the Steady State Model, Eqs. (21), (22), for different inlet pressures, P_{in}, as indicated by color. *Solids lines* are from the simulations, and symbols are data from Pong et al. [16]. (**a**) Darcy's law, Case 1 in Table 2, with compressibility factors, $\zeta_\gamma = 0$. (**b**) Civan's model with constant compressibility factors, $\zeta_\gamma = Const$, for some parameters, see [7]. (**c**) Case 16 in Table 2 (new model) with pressure dependent parameters and non-constant compressibility factors, $\zeta_\gamma(p)$. (**d**) Relative errors for the 16 cases in Table 2

Table 3 Reservoir model parameters used in the Base Case, Case 16 in Table 2

Parameter		Parameter	
L (m)	0.003	α_{KC}	1
N_x	100	β_{KC}	1
R_g (J kmol^{-1} K^{-1})	8314.4	Γ_{KC}	1
M_g (kg kmol^{-1} K^{-1})	16	a_ϕ	0.2
T (K)	350	b_ϕ	-1×10^{-6}
p_c (kPa)	3.1×10^3	c_ϕ	1.96
t_c (K)	125	σ_0	10
b_{SF}	-1	A_σ	0.2
a_τ	1.5	B_σ	0.4

Table 4 The range of parameters that are used to determine the values of permeability, and porosity in Fig. 3, from Eqs. (2) and (3)

Cases	α_{KC}	β_{KC}	Γ_{KC}	a_ϕ	b_ϕ	c_ϕ
1	1.0	1.0	1.0	0.20	−1e−6	1.96
2	1.0	0.65	1e−7	0.08	−1e−6	2.09
3	0.75	0.66	1e−7	0.15	−1e−6	2.09
4	0.25	0.4	1e−8	0.15	−1e−6	1.96
5	0.5	0.5	0.1	0.10	−1e−6	2.1112
6	0.5	1.5	1.0	0.05	−1e−8	2.90
7	0.45	0.65	1e−6	0.01	−1e−8	2.88

$K = 1 \times 10^{-15}$ m^2. From the present calculations the porosity is pressure dependent and in the range $0.01 \leq \phi \leq 0.2$, and the permeability is also pressure dependent and in the range $10^{-20} \leq K \leq 10^{-3}$ m^2, which are more realistic (Table 4).

5 Sensitivity Analysis and Estimation of Model Parameters

It is important to determine how much the results and predicted rock properties change due to small changes in model parameters. A sensitivity analysis was carried out by adjusting one model parameter at a time by factors of 2 and $1/2$, starting with Case 16 as the base case – One-at-a-Time (OAT) methodology. Sensitivity is measured by monitoring the changes in the model output.

Figure 2 shows sensitivity to selected parameters: (a) p_c (critical pressure), (b) T (temperature), (c) a_τ (constant in the tortuosity model), (d) a_ϕ (constant in the porosity model). Except for the temperature, Fig. 2b, all results show significant sensitivity to changes in the selected parameter especially at higher inlet pressures.

Figure 3 illustrates the sensitivity of the calculated permeability, and porosity against the pressure, for different combinations of α_{KC}, β_{KC}, and Γ_{KC}, Eq. (2).

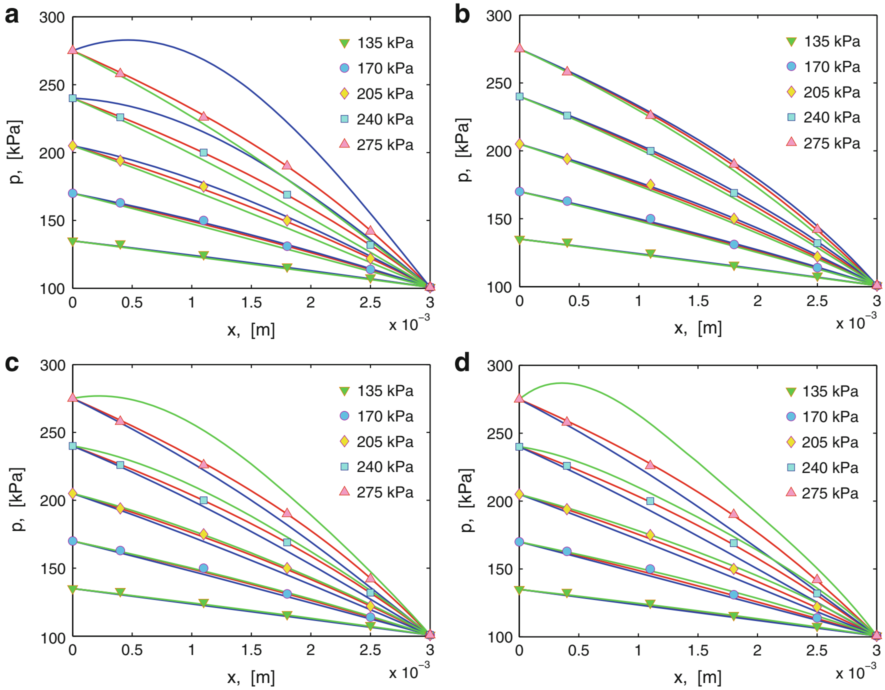

Fig. 2 OAT sensitivity analysis of the new model. Symbols are the data from Pong et al. [16] (see Fig. 2 for details). Sensitivity to the following parameters: (**a**) Critical pressure p_c, (**b**) Temperature T, (**c**) Tortuosity parameter a_τ in Eq. (3), (**d**) porosity parameter a_ϕ in Eq. (4). *Red lines* are the Base Case parameter values in Table 3. *Blue lines*: the specific parameter is divided by 2. *Green lines*: the specific parameter is multiplied by 2

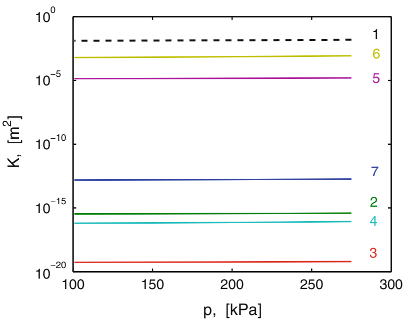

(a) Permeability

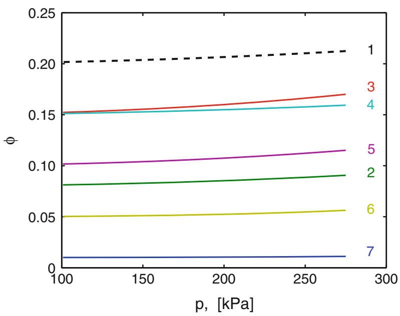

(b) Porosity

Fig. 3 Permeability (K), and porosity (ϕ), against the pressure p, based upon the parameter values in Table 3. Seven cases for each parameter, shown in Table 4, are considered and are indicated on the plots. (Case 1 is the Base Case, shown as *black dashed line*.) (**a**) permeability curves are obtained using data from columns 2 to 4 of Table 4. (**b**) Porosity curves are obtained using data from columns 5 to 7

6 Summary

The Base Case 16 in Table 2, which is the fully pressure-dependent non-linear model, performs better than other models giving the smallest error against available data, Fig. 1c. Darcy's Law performs the worst illustrating its limitations for gas transport in tight porous media. A OAT sensitivity analysis shows that rock properties such as the porosity, and permeability, are very sensitive to most of the model parameters, Figs. 2 and 3. In the future, the sensitivity analysis for all of the model parameters will be completed.

Acknowledgements The authors would like to acknowledge the support provided by King Abdulaziz City for Science and Technology (KACST) through the Science Technology Unit at King Fahd University of Petroleum and Minerals (KFUPM) for funding this work through project No. 14-OIL280-04.

References

1. Ali, I., Malik, N.A., Chanane, B.: Time-fractional nonlinear gas transport equation in tight porous media: an application in unconventional gas reservoirs. In: 2014 International Conference on Fractional Differentiation and Its Applications (ICFDA), Catania, pp. 1–6. IEEE (2014)
2. Aziz, K., Settari, A.: Petroleum Reservoir Simulation, vol. 476. Applied Science Publishers, London (1979)
3. Beskok, A., Karniadakis, G.E.: Report: a model for flows in channels, pipes, and ducts at micro and nano scales. Microsc. Thermophys. Eng. **3**(1), 43–77 (1999)
4. Carman, P.C., Carman, P.C.: Flow of Gases Through Porous Media. Butterworths Scientific Publications, London (1956)
5. Chen, Z.: Reservoir Simulation: Mathematical Techniques in Oil Recovery. CBMS-NSF Regional Conference Series in Applied Mathematics, vol. 77. SIAM, Philadelphia (2007)
6. Civan, F.: Effective correlation of apparent gas permeability in tight porous media. Transp. Porous Media **82**(2), 375–384 (2010)
7. Civan, F., Rai, C.S., Sondergeld, C.H.: Shale-gas permeability and diffusivity inferred by improved formulation of relevant retention and transport mechanisms. Transp. Porous Media **86**(3), 925–944 (2011)
8. Civan, F., et al.: Improved permeability equation from the bundle-of-leaky-capillary-tubes model. In: SPE Production Operations Symposium, Oklahoma City. Society of Petroleum Engineers (2005)
9. Cui, X., Bustin, A., Bustin, R.M.: Measurements of gas permeability and diffusivity of tight reservoir rocks: different approaches and their applications. Geofluids **9**(3), 208–223 (2009)
10. Cussler, E.L.: Diffusion: Mass Transfer in Fluid Systems. Cambridge University Press, Cambridge/New York (2009)
11. Darishchev, A., Rouvroy, P., Lemouzy, P.: On simulation of flow in tight and shale gas reservoirs. In: 2013 SPE Middle East Unconventional Gas Conference & Exhibition, Muscat (2013)
12. Kumar, N.: Compressibility factors for natural and sour reservoir gases by correlations and cubic equations of state. M.Sc. Thesis, Texas Tech University (2004)
13. Loeb, L.B.: The Kinetic Theory of Gases. Courier Dover Publications (2004)

14. Mahmoud, M.: Development of a new correlation of gas compressibility factor (z-factor) for high pressure gas reservoirs. J. Energy Resour. Technol. **136**(1), 012903 (2014)
15. Peaceman, D.W.: Fundamentals of Numerical Reservoir Simulation. Elsevier, New York (1977)
16. Pong, K.C., Ho, C.M., Liu, J., Tai, Y.C.: Non-linear pressure distribution in uniform microchannels. ASME public. FED **197**, 51–51 (1994)
17. Rathakrishnan, E.: Gas Dynamics. PHI Learning, New Delhi (2013)
18. Wang, Z., Krupnick, A.: A retrospective review of shale gas development in the United States. What led to the boom? Pub. Resources, Washington (2013)
19. Ziarani, A.S., Aguilera, R.: Knudsen's permeability correction for tight porous media. Transp. Porous Media **91**(1), 239–260 (2012)

Solutions of Time-Fractional Diffusion Equation with Reflecting and Absorbing Boundary Conditions Using Matlab

Iftikhar Ali, Nadeem A. Malik, and Bilal Chanane

Abstract The main objective of this work is to develop Matlab programs for solving the time-fractional diffusion equation (TFDE) with reflecting and absorbing boundary conditions on finite and infinite domains. Essentially, there are three major codes, one for finding the exact solution of the TFDE and other two are for finding the numerical solution of the TFDE. The code for finding the exact solutions is based on the fundamental solution of the TFDE, whereas the codes for finding the numerical solutions are based on the explicit and the implicit finite difference schemes, respectively. Finally, we illustrate the effectiveness of the codes by applying them to TFDEs with sharp initial data and for various reflecting and absorbing boundary conditions both on finite and infinite domains. The results show the difference of solutions between the standard diffusion equation and the time-fractional diffusion equation.

1 Introduction

Many physical processes evolve in spaces that are heterogeneous in nature, such as, crowded system, protein diffusion within cells, anomalous diffusion through porous media, see [3, 4, 6, 17]. Mathematical models, based on standard calculus, have failed to describe such intricate processes whereas mathematical models, based on fractional calculus techniques, have proven their effectiveness in explaining such complex processes, [1, 2, 5, 10, 15].

Time-fractional diffusion equation have been derived in the framework of Continuous Time Random Walk (CTRW) model. It is based on the idea of considering the transport processes as the flow of particles in the form of packets and then assigning a probability of locating a packet at position x at time t. Law of Total Probability is used to determine probability $P(x,t)$. Luchko has derived the time-fractional diffusion equation by using these concept, see the details in [8, 9]. The

I. Ali (✉) • N.A. Malik • B. Chanane
King Fahd University of Petroleum and Minerals, Dhahran, Saudi Arabia
e-mail: iali@kfupm.edu.sa

J. Bélair et al. (eds.), *Mathematical and Computational Approaches in Advancing Modern Science and Engineering*, DOI 10.1007/978-3-319-30379-6_2

equation is given by,

$$\tau \partial_t P(x,t) = \partial_t^{1-\alpha}[-v\partial_x P(x,t) + k^2\partial_x^2 P(x,t)] \tag{1}$$

as $t \to \infty$ and $|x| \to \infty$. Equation (1) is called time-fractional advection-diffusion equation and in the case $v = 0$ it reduces to time-fractional diffusion equation. For more detailed derivation, see [9, 11].

In this work, we develop Matlab programs for finding exact and numerical solutions of the time fractional diffusion equation (TFDE) on finite and infinite domains, and also with various boundary conditions. The manuscript is organized as follows; in Sect. 2, procedure for finding the fundamental solution of the TFDE is explained; in Sect. 3, the numerical schemes are discussed; in Sect. 4, Matlab codes are provided; in Sect. 5, several examples are given to illustrate the effectiveness of Matlab programs; finally, in Sect. 6, conclusions are given.

2 Fundamental Solution of Time Fractional Diffusion Equation

Consider the time fractional diffusion equation, in Caputo form, over the whole real line with given initial data,

$$\frac{\partial^\alpha}{\partial t^\alpha}u(x,t) = \frac{\partial^2}{\partial x^2}u(x,t), \qquad 0 < \alpha \le 1 \tag{2}$$

$$u(x,0) = f(x). \tag{3}$$

Equation (2) can be written in the integral form as follows,

$$u(x,t) = f(x) + \frac{1}{\Gamma(\alpha)}\int_0^t (t-\tau)^{\alpha-1}u_{xx}(x,\tau)d\tau. \tag{4}$$

Application of Laplace transform yields a second order linear differential equation

$$\tilde{u}_{xx}(x,p) - p^\alpha \tilde{u}(x,p) = -f(x)p^{\alpha-1}. \tag{5}$$

The solution of Eq. (5) is given by

$$\tilde{u}(x,p) = \int_{-\infty}^{\infty} \tilde{k}(|x-y|, p^{\alpha/2})p^{\alpha-1}f(y)dy, \tag{6}$$

where $k(|x|,\lambda) = \frac{1}{\sqrt{2\pi\lambda}}|x|^{1/2}k_{1/2}(\lambda|x|)$ is modified Bessel function of second kind [16]. Furthermore, Eq. (6) can be expressed as

$$\tilde{u}(x,p) = \int_{-\infty}^{\infty} \tilde{G}^{\alpha}(|x-y|,p)f(y)dy, \tag{7}$$

where $\tilde{G}^{\alpha}(|x|,p) = \tilde{k}(|x|,p^{\alpha/2})p^{\alpha-1}$.

Note that directly taking the inverse Laplace transform is not feasible, so we use the relationship between the Laplace and Mellin transforms to obtain

$$\begin{aligned}\tilde{G}^{\alpha}(|x|,s) &= \frac{1}{\Gamma(1-s)}\int_0^{\infty} p^{-s}\tilde{G}^{\alpha}(|x|,p)dp \\ &= \frac{|x|^{1/2}}{\sqrt{2\pi}\Gamma(1-s)}\int_0^{\infty} p^{3\alpha/4-s-1}\tilde{k}_{1/2}(|x|p^{\alpha/2})dp.\end{aligned} \tag{8}$$

Using the results,

$$\mathscr{M}[x^{\lambda}f(ax^b)] = \frac{1}{b}a^{-\frac{s+\lambda}{b}}\tilde{f}\left(\frac{s+\lambda}{b}\right),$$

$$\tilde{k}_{\sigma}(s) = 2^{s-2}\Gamma\left[\frac{s-\sigma}{2}\right]\Gamma\left[\frac{s+\sigma}{2}\right],$$

Equation (8) becomes

$$\tilde{G}^{\alpha}(|x|,s) = \frac{1}{\alpha\sqrt{\pi}}2^{-2s/\alpha}|x|^{2s/\alpha-1}\frac{\Gamma[1-s/\alpha]\Gamma[1/2-s/\alpha]}{\Gamma[1-s]}. \tag{9}$$

Taking the inverse Mellin transform and using Fox function, we obtain

$$G^{\alpha}(|x|,t) = \frac{1}{\alpha\sqrt{\pi}}|x|^{-1}H_{12}^{20}\left[\frac{|x|^{2/\alpha}}{2^{2/\alpha}t}\left|\begin{matrix}(1,1)\\(1/2,1/\alpha),(1,1/\alpha)\end{matrix}\right.\right]. \tag{10}$$

The general solution of the time fractional diffusion equation is given by

$$u(x,t) = \int_{-\infty}^{\infty} G^{\alpha}(|x-y|,t)f(y)dy. \tag{11}$$

If the initial data is given as delta potential, that is, $u(x,0) = \delta(x)$, then the solution (11) becomes

$$u(x,t) = \frac{1}{\alpha\sqrt{\pi}}|x|^{-1}H_{12}^{20}\left[\frac{|x|^{2/\alpha}}{2^{2/\alpha}t}\left|\begin{matrix}(1,1)\\(1/2,1/\alpha),(1,1/\alpha)\end{matrix}\right.\right]. \tag{12}$$

For more details, readers are referred to Wyss [18] and Schneider & Wyss [14].